

A new ornithurine from the Early Cretaceous of China sheds light on the evolution of early ecological and cranial diversity in birds

Jiandong Huang, Xia Wang, Yuanchao Hu, Jia Liu, Jennifer A Peteya, Julia A. Clarke

Despite the increasing number of exceptional feathered fossils discovered in the Late Jurassic and Cretaceous of northeastern China, representatives of Ornithurae, a clade that includes comparatively-close relatives of crown clade Aves (extant birds) and that clade, are still comparatively rare. Here, we report a new ornithurine species *Changzuiornis ahgmi* from the Early Cretaceous Jiufotang Formation. The new species shows an extremely elongate rostrum so far unknown in basal ornithurines and changes our understanding of the evolution of aspects of extant avian ecology and cranial evolution. Most of this elongate rostrum in *Changzuiornis ahgmi* is made up of maxilla, a characteristic not present in the avian crown clade in which most of the rostrum and nearly the entire facial margin is made up by premaxilla. The only other avialans known to exhibit an elongate rostrum with the facial margin comprised primarily of maxilla are derived ornithurines previously placed phylogenetically as among the closest outgroups to the avian crown clade as well as one derived enantiornithine clade. We find that, consistent with a proposed developmental shift in cranial ontogeny late in avialan evolution, that this elongate rostrum is achieved through elongation of the maxilla while the premaxilla remains only a small part of rostral length. Thus, only in Late Cretaceous ornithurine taxa does the premaxilla begin to play a larger role. The rostral and postcranial proportions of *Changzuiornis* suggest an ecology not previously reported in Ornithurae; the only other species with an elongate rostrum are two marine Late Cretaceous taxa interpreted as showing a derived picivorous diet.

1 **A new ornithurine from the Early Cretaceous of China sheds light on the evolution of early**
2 **ecological and cranial diversity in birds**

3 **Jiandong Huang¹, Xia Wang², Yuanchao Hu¹, Jia Liu¹, Jennifer Peteya³ and Julia A.**

4 **Clarke²**

5 ¹ Anhui Geological Museum, Hefei, Anhui 230031, China

6 ²Department of Geological Sciences, Jackson School of Geoscience, University of Texas,
7 Austin, TX 78712,

8 ³Department of Biology & Integrated BioScience Program, University of Akron, Akron, OH
9 44325-390

10

11 Corresponding authors: wangxia8383@gmail.com; julia_clarke@jsg.utexas.edu

12

13 **ABSTRACT**

14

15 Despite the increasing number of exceptional feathered fossils discovered in the Late Jurassic and
16 Cretaceous of northeastern China, representatives of Ornithurae, which includes close relatives of
17 crown clade Aves (extant birds) and that clade, are still comparatively rare. Here, we report a new
18 ornithurine species *Changzuiornis ahgmi* from the Early Cretaceous Jiufotang Formation. The new
19 species shows an elongate rostrum so far unknown in basal ornithurines and changes our
20 understanding of the evolution of aspects of extant avian ecology and cranial evolution. Most of
21 this elongate rostrum in *Changzuiornis ahgmi* is made up of maxilla, a characteristic not presents
22 in the avian crown clade in which most of the rostrum and nearly the entire facial margin is made
23 up by premaxilla. We find that, consistent with a proposed developmental shift to elongated
24 rostrum in cranial ontogeny late in avialan evolution, that this elongate is achieved through
25 elongation of the maxilla while the premaxilla remains only a small part of rostral length, and only
26 in Late Cretaceous ornithurine taxa does the premaxilla begin to play a larger role. The rostral and
27 postcranial proportions of *Changzuiornis* suggest ecology not previously reported in early
28 Ornithurae.

29

30 **Keywords** Avialae, fossil, ontogeny, Ornithurae, Jehol Biota

31

32 **INTRODUCTION**

33

34 So far more than 14 species of ornithurine birds have been reported from an array of localities of
35 the Early Cretaceous of northern China, Jehol Biota (Fig.1) Only six are (i.e., *Yanornis martini*,
36 *Gansus yumenensis*, *Hongshanornis longicresta*, *Archaeorhynchus spathula*, *Iteravis*
37 *huchzermeyeri* and *Gansus zheni*) represented by multiple specimens. The majority of taxa are
38 known from the Jiufotang Formation (122.1±0.3 Ma, Chang et al., 2009) of Western Liaoning
39 Province, China with *Archaeorhynchus* is known from both the older Yixian Formation as well
40 as the Jiufotang Formation. *Archaeornithura meemanae* is the oldest taxon in the
41 Hongshanornithidae; it is known from the Huajiying Formation (Wang et al., 2015). Most
42 Chinese ornithurines have been proposed to be volant and semi-aquatic, with *Gansus*
43 *yumenensis*, known from the Xiagou Formation (early Aptian, Suarez et al., 2013), proposed to

44 likely represent a foot-propelled diver (You et al., 2006; Nudds et al., 2013). Some more basal
45 taxa placed outside of Ornithurae (e.g., *Jianchangornis microdonta* and *Archaeorhynchus*
46 *spathula*), have been proposed to have occupied fully terrestrial niches (Zhou et al., 2009; Zhou
47 et al., 2013). However, despite the ever increasing number of avialan specimens discovered from
48 China, Early Cretaceous birds were found to be substantially impoverished in ecology (Mitchell
49 & Makovicky, 2014).

50

51 Known diversity in rostral shape of these Jehol taxa has also been limited; the majority have
52 relatively short rostra and the only other bird with an elongate rostrum proposed to be part of
53 Ornithurae is *Xinghaiornis lini*, from the Yixian Formation (Wang et al., 2013). Here, we
54 describe and evaluate the phylogenetic position of a new ornithurine species with an elongate
55 rostrum and gastroliths from a relatively new locality (Sihedang), Early Cretaceous, Jiufotang
56 Formation of Liaoning Province. This species contributes to our understanding of Mesozoic
57 avialan cranial diversity and evolution.

58 The electronic version of this article in Portable Document Format (PDF) will represent a
59 published work according to the International Commission on Zoological Nomenclature (ICZN),
60 and hence the new names contained in the electronic version are effectively published under that
61 Code from the electronic edition alone. This published work and the nomenclatural acts it
62 contains have been registered in ZooBank, the online registration system for the ICZN. The
63 ZooBank LSIDs (Life Science Identifiers) can be resolved and the associated information viewed
64 through any standard web browser by appending the LSID to the prefix "http://zoobank.org/".
65 The online version of this work is archived and available from the following digital repositories:
66 PeerJ, PubMed Central and CLOCKSS.

67

68 SYSTEMATIC PALEONTOLOGY

69 Aves Linnaeus, 1758

70 Ornithurae Haeckel, 1866 sensu Gauthier and de Queiroz 2001

71 *Changzuiornis ahgmi* gen. et sp. nov.

72

73 **Holotype specimen.** A nearly-complete skeleton with feather impressions (Figs.2-3; AGB5840;
74 "AGB" refers to the Anhui Gushengwu Bowugan in pinyin, or Anhui Paleontological Museum,
75 which is the Anhui Geological Museum). The skeleton is preserved primarily in lateral view. Parts
76 of the pectoral and pelvic girdles are partially disarticulated as are some of the manual phalanges
77 and caudal vertebrae.

78

79 **Locality and horizon.** Sihedang locality, Lingyuan City, western Liaoning Province, China.
80 Jiufotang Formation, Early Cretaceous (Aptian; Chang et al., 2009).

81

82 **Etymology:** The genus name derives from Chinese pinyin "Changzui" referencing the long beak
83 and Greek word "ornis-" for bird; and the species name refers to Anhui Geological Museum
84 (AHGM) where the holotype specimen is housed.

85

86

87 **Diagnosis**

88 The placement of *Changzuiornis ahgmi* within the clade Ornithurae is supported by seven
89 unambiguously optimized synapomorphies (listed in the Phylogenetic Analysis section below). It
90 diagnosed by a combination of morphologies not seen in other described ornithurines: The rostrum
91 is elongate, comprising greater than 60% of the total skull length. Most of this elongate rostrum is
92 made up of maxilla, a characteristic not present in the avian crown clade in which most of the
93 rostrum and nearly the entire facial margin is made up by premaxilla. The only other avialans
94 known to exhibit an elongate rostrum with the facial margin comprised primarily of maxilla are
95 *Xinghaiornis* and derived Late Cretaceous ornithurines previously placed phylogenetically as
96 among the closest outgroups to the avian crown clade (i.e., *Ichthyornis*, hesperornithine taxa). It
97 differentiated from *Xinghaiornis* by its much smaller size, many tiny teeth on the lower jaw, U-
98 shaped furcula, metacarpal III sub-equal to metacarpal II in distal extent, a carpometacarpus with
99 both proximal and distal fusion, and a tarsometatarsus that is completely fused. The new species
100 is differentiated from Hesperornithes and *Ichthyornis* by significantly smaller teeth with less
101 recurved crowns, the presence of a distinct dorsal process or “forking” of the posterior dentary,
102 and the presence of a pubic symphysis. It is additionally differentiated from *Ichthyornis* by robust
103 and more abbreviate furcular rami, a narrower sternal margin of the coracoid, and a significantly
104 more elongate scapular acromion.

105

106 **DESCRIPTION**

107 **Skull**

108 The skull (Fig. 3) is preserved in right lateral view. The rostrum is elongate (48mm), comprising
109 ~68% of the total skull length. It is longer than those reported in the only other long-rostrum
110 Jehol taxa, the longipterygid enantiornithines, *Longipteryx* (64%), *Rapaxavis pani* (65%),
111 *Longirostravis* (60%-64%) and *Shanweinia* (62%), and comparable in proportions to those of
112 extant woodcocks. The dorsal processes of the premaxillae are not fused to each other posteriorly
113 (Fig. 4). While the right dorsal process is missing, the left one visibly extends posteriorly to
114 contact the frontal. The posterior tip of the facial margin of the left premaxilla is missing while
115 the articulating tip of the maxilla is visible and sharply tapered rostrally (Fig. 4). From the length
116 of the exposed maxilla, the premaxilla comprised less than one half of the facial margin
117 (rostrum), a condition also seen in enantiornithines with long rostra (e.g., *Longirostravis* and
118 *Shanweinia*; Hou et al., 2004; O'Connor et al., 2009).

119 The right nasal is laterally exposed with a descending process that lies adjacent to a small dorsal
120 process of the maxilla (Fig.4). The nasals appear not to have contacted along the dorsal midline
121 but were likely separated by the frontal processes of the premaxillae as seen in *Confuciusornis*
122 (Chiappe et al., 1999; Fig. 3) or underlay parts of these processes. However, the right nasal does
123 not appear preserved in life position. The external nares are elongate and relatively narrow. A
124 thin vertical sheet-like element visible in the narial region extends the length of the external
125 nares and is interpreted as an internarial septum (Figs. 3, 4). The preservation of an internarial
126 septum in *Changzuiornis* is the first known occurrence in a Mesozoic bird. A similar sheet like
127 element is visible below several the preserved scleral ossicles, consistent with at least a partial
128 interorbital septum formed by the mesethmoid; Fig. 4). A mesethmoid is present in an array of
129 basal avialans including *Confuciusornis* and ornithurines such as *Yixianornis* as well as

130 Enantiornithes (e.g., *Longipteryx haoyangensis* and *Schizooura lii*; Zhou & Zhang, 2001; Clarke
131 et al., 2006; Zhou et al., 2012).

132

133 Parts of the rostral jugal and posterior-most quadratojugal are preserved. Just dorsal to the small
134 rostral portion of the jugal (preserved at its contact with the maxilla), the poorly preserved
135 remnants of the right lacrimal are visible (Fig. 3). The quadrate is poorly preserved but shows an
136 arcuate posterior margin and a relatively elongate orbital process (Fig. 3). The frontoparietal
137 suture appears to have been open (Fig. 3). The posterior portion of the skull is severely crushed.
138 A small roughly t-shaped element preserved nearly the posterior margin of the orbit could
139 represent a remnant of a postorbital; however, this cannot be ascertained with confidence and a
140 postorbital is currently unknown in Ornithurae (Martin, 2011).

141 The mandibles are relatively straight and taper anteriorly. A prementary bone lies in front of left
142 mandibular ramus (Fig. 3). Such a structure has also been reported in *Hongshanornis*.

143 *Ichthyornis*, *Hesperornis*, and *Parahesperornis* and an array of other ornithurine birds (e.g.,
144 Zhou & Zhang, 2005). The dentary is forked posteriorly whereas the posterior dentary lacks a
145 dorsal process in *Ichthyornis* and *Hesperornithes* (Fig.4). At least three large mental foramina are
146 visible in a shallow groove near the dorsal margin of the rostral dentary. The mandible is
147 obscured by partly crushing posterior to the dentary.

148 Both premaxillae are completely edentulous, unlike those in the enantiornithines *Longipteryx*,
149 *Rapaxavis*, *Longirostravis* and *Shanweinia* (O'Connor & Chiappe, 2011). Approximately
150 seven tiny, narrow, pointed and unserrated loose teeth are exposed closely between the maxilla
151 and dentary (Fig. 3). One appears to be in situ, indicating an association with the dentary. No
152 teeth seem preserved on the tip of dentary. Small neurovascular foramina are visible on the
153 dorsal surface of the premaxilla consistent with the presence of a rhamphotheca (e.g., Chiappe et
154 al., 1999).

155 Parts of the hyoid elements are preserved. Two recurved ceratobranchials are preserved with
156 breakage separating their rostral-most tips from the rest of their preserved length. These rostral
157 tips lie close to the right mandible (Fig. 3). A small, isolated element preserved below their tips
158 may comprise a very small, ossified basihyal (Fig. 3: bh).

159 **Vertebral column**

160 The entire cervical series is preserved. The anterior cervicals are visibly heterocephalic while
161 posterior-most cervicals do not appear heterocephalic, but are poorly exposed. The mid-series
162 (fifth- eighth) cervical vertebrae are elongate. Elongate costal processes are present on the
163 second through eighth vertebrae of the eleven or twelve vertebrae in the series (Fig. 2). The
164 thoracic series is obscured by the right scapula. However, approximately ten thoracic vertebrae
165 are discernable with large lateral fenestrae (Fig. 2) and amphiplatyan centra articulations. The
166 neural spines are craniocaudally elongate. The sacrum is badly crushed, and no morphologies
167 can be discerned. Only the approximate outlines of several free caudal vertebrae are visible while
168 the pygostyle is clearly exposed. It is strongly mediolaterally compressed and short,
169 approximately two anterior caudal vertebrae in length (Fig. 2).

170 **Pectoral girdle and limb**

171 The right coracoid is exposed in ventral view (Fig. 2). The left coracoid is obscured by the
172 furcula and the right humerus. A large flange-like procoracoid process and an abbreviated lateral
173 process are present (Fig.5). The furcula is U-shaped and relatively thin; a furcular apophysis
174 appears to be absent. The omal tips of the rami are severely crushed. The left scapula, lying
175 under the furcula and several ribs, preserves an elongate and hook-shaped acromion process
176 (Fig.5). The posterior ends of both scapulae are missing. However, their preserved length
177 approaches that of the humeri. The sternum is not visible. Approximately five large gastroliths
178 (~30mm in diameter; Fig. 2) are visible in the abdominal region, between the coracoid and the
179 posterior thoracic vertebrae. A small quantity of fine grit is intermixed with these larger stones.
180 Unfortunately, a textured depression just posterior to the five preserved stone may indicate a
181 larger quantity of such stones were present but lost during collection or early preparation.

182 Both humeri are exposed in anterior view (Figs. 2, 5), and are just slightly shorter than the ulnae.
183 The dorsally-directed deltopectoral crest is recurved and projected approximately equal to shaft
184 width (Fig.5). It extends distally for just greater than 1/3 of the total humeral length and then
185 grades gently into the shaft. The head is weakly globose, and a small m. acrocoracohumeralis
186 ligament scar is visible. On the distal humerus, the dorsal condyle is more elongate than the
187 ventral. The radii are narrower than the slightly-bowed ulnae. Few morphologies of the proximal
188 or distal radii and ulnae are visible. The radiale is larger than the ulnare, and the ulnare appears
189 differentiated into distinct dorsal and ventral rami.

190 The right carpometacarpus is exposed in dorsal view and the left, in ventral view. The
191 metacarpals are fused proximally and distally. Metacarpal III is significantly narrower than
192 metacarpal II. It is straight and closely appressed to metacarpal II. On the left carpometacarpus, a
193 small piciform process is visible (Fig. 6). Metacarpal I bears a very weakly-projected extensor
194 process (Fig.6); its anterior margin is nearly straight. Digit I:1 extends over ½ the length of
195 metacarpus and bears a small claw. Manual digit II:1 is approximately the same length as digit
196 II:2. The posterior margin of digit II:1 is strongly compressed dorsoventrally, and digit II:2
197 shows a distinct fossa that in crown clade Aves is the attachment site for the leading edge
198 primary feather (Fig.6; Hieronymus, 2015). An impression of a small digit II unguis is preserved
199 on the left side. It is only weakly recurved. Phalanx III:1 is not visible.

200 **Pelvic girdle and limb**

201 Most of the partially-disarticulated pelvic girdle is obscured by crushing. The rod-like pubes
202 (Figs. 2, 7) have separated from the rest of the pelvic elements and preserve a relatively elongate
203 symphysis. Their distal ends are not visibly expanded. The femur is notably shorter than the
204 tarsometatarsus (Table 1) and its shaft is straight. The trochanteric crest is weakly projected
205 proximally. The attachment of the capital ligament is indicated by a distinct notch on the lateral
206 surface of the proximal femur (Fig.7). The left tibia preserves a slightly proximally-projected
207 anterior cnemial crest (Fig. 7). The morphology of the distal condyles is poorly preserved, but
208 they appear fused to the tibia and are visibly separated by an intercondylar incisure (Fig.7). The
209 distal tarsals are fused to the metatarsals.

210 The tarsometatarsus is mediolaterally compressed. A prominent midline m. tibialis cranialis
211 tubercle is visible on the proximodorsal left tarsometatarsus (Fig. 7). The j-shaped metatarsal I is

212 well-exposed in articulation with a short hallux; pedal digit I:1 is longer than the small ungual,
213 I:2. Pedal phalanges are preserved in association with both tarsometatarsi. They are narrow with
214 deep flexor pits and only weakly recurved unguals. In all digits (Fig. 2), the unguals are shorter
215 than their penultimate phalanges. The flexor tubercles on the unguals are proximally located,
216 unlike the more distally located tubercles used to infer the presence of webbing in *Gansus*
217 *yumenensis* (You et al., 2006). In digit II, the second phalanx slightly exceeds the first in length.
218 Both non-terminal phalanges of this digit are the longest of the pedal digits. In digit three, the
219 penultimate phalanx is slightly shorter than the more proximal phalanges. By contrast, in the
220 fourth digit, the penultimate phalanx is slightly longer than the more proximal phalanges.

221 **Feathers**

222 Feather remains are poorly preserved (Fig. 2). Remnants of body contour feathers are associated
223 with the posterior cranium and the cervical area as well as near wing and leg elements. In
224 addition, several primary feathers are associated with both forelimbs. Traces of rachis and barbs
225 are distinguishable only in certain distal regions of these feathers, which are otherwise preserved
226 as grey-white impressions. One primary feather associated with left manual digit II:1 is
227 approximately 106 mm in length. The rachis of this asymmetrically veined feather is discernable.
228 The lengths of the rest of the preserved remiges are impossible to determine with confidence.
229 Scanning electron microscopy (SEM) results show that wing and leg/tail feather samples contain
230 melanosome molds that are highly aligned, closely spaced and elongate in shape (Fig.2). Their
231 aspect ratio (length:width ratio:2.29-4.99) is typical of eumelanosomes seen in black feathers
232 (Vinther et al., 2009; Li et al., 2010; Clarke et al., 2010).

233 **Maturity**

234 The following anatomical features present the holotype specimen have been proposed to indicate
235 an adult at death (Forster et al., 1998; Xu & Norell, 2004; Turner et al., 2007; Gao et al., 2012;
236 Godefroit et al., 2013): (i) the texture of the bones is regular and well ossified bearing articular
237 facets and muscular scars (e.g., proximal and distal ends of the coracoid, the humerus, the ulna,
238 the pubis and the femur); (ii) the frontals are fused to each other; (iii) cervical ribs and cervical
239 vertebrae co-ossified to enclose transverse foramina; (iv) distal carpals coossified with
240 metacarpals II and III; (v) metatarsals II, III and IV fused throughout their length.

241 **PHYLOGENETIC ANALYSIS**

242 We investigated the phylogenetic position of *Changzuiornis* using a dataset of 220 morphological
243 characters modified from that of Li et al. (2014). This dataset (Appendix I and II) was revised by
244 modifying and ordering one character (relative length of pedal digits; character 217; Appendix I)
245 and adding *Gansus yumenensis*. All analyses were performed using PAUP 4.0b10 (Swofford,
246 2003). Heuristic searches were used given the size of the taxonomic sample (40 ingroup and
247 outgroup taxa). Three thousand replicates of random stepwise addition (branch swapping: tree-
248 bisection-reconnection) were performed holding only one tree at each step. Branches were
249 collapsed to create polytomies if the minimum branch length was equal to zero. One thousand
250 bootstrap replicates with ten random stepwise addition heuristic searches per replicate were also
251 performed with the same settings as in the primary analysis. Bootstrap support for those nodes
252 recovered in greater than 50 percent of the 500 replicates performed and Bremer support values

253 are reported to the right of the node to which they apply (Format: Bootstrap/Bremer in Fig. 8).
254 Bremer support values were calculated by iterative searches for suboptimal trees in PAUP 4.0b10
255 using the same heuristic search strategy as the primary analysis. 15 most parsimonious trees
256 (MPTs) were recovered (L=585, CI=0.50, RI=0.79, RC=0.40; PIC only).

257

258 The strict consensus tree (Fig.8) recovers *Changzuiornis ahgmi* within Ornithurae closer to Aves
259 than the clade formed by *Yixianornis*, *Songlingornis* and *Yanornis* but basal to *Gansus*
260 *yumenensis* and the clade *Gansus zheni*+*Iteravis*. The later clade is supported by one
261 unambiguous synapomorphy, a reversal (170:0, distal end of pubes expanded or flared). The
262 placement of *Changzuiornis ahgmi* within Ornithurae is supported by seven unambiguously
263 optimized synapomorphies (numbers refer to characters and states listed in Appendix II): 9:1,
264 nasal process of premaxilla long, closely approaching frontal; 87:1, coracoid, procoracoid
265 process present; 140:3, semilunate carpal and metacarpals complete proximal and distal fusion;
266 142:1, metacarpal III, anteroposterior diameter as a percent of same dimension of metacarpal II
267 less than 50%; 151:1, manual digit II, phalanx 1 strongly dorsoventrally compressed, flat caudal
268 surface; 192:1, metatarsal III proximally displaced plantarly, relative to metatarsals II and IV;
269 218:1, hallux, claw to phalanx proportions, 1:1, shorter. Unlike previous studies (e.g., Clarke &
270 Norell, 2002; Clarke, 2004; Clarke et al., 2006; Zhou et al., 2008; O'Connor et al., 2010),
271 *Apsaravis* is placed more closely to Aves than *Ichthyornis*, which is supported by six
272 unambiguous synapomorphies (4:1, dentary teeth absent; 6:1, dentaries joined by a bony
273 symphysis; 52:2, cervical vertebrae with heterocoelous anterior and posterior centra; 204:1,
274 metatarsal II shorter than metatarsal IV, but reaching distally farther than the base of the
275 metatarsal IV trochlea; 212:1, over half of the glenoid facet lies omal to the cotyla in lateral
276 view). The skull characters (especially characters of the dentition) are missing data in *Gansus*
277 *yumenensis*, which may influence this optimization. Indeed, when we remove *Gansus*
278 *yumenensis* from the phylogenetic analysis, *Apsaravis* is placed as basal to *Ichthyornis* +
279 *Hesperornithes* as in all previous analyses (e.g., Clarke, 2004; Clarke et al., 2006; Zhou et al.,
280 2008; O'Connor et al., 2010; Zhou et al., 2012; Li et al., 2014). *Apsaravis* shares loss of teeth
281 with Aves, a highly homoplastic character in Avialae, but lacks features seen in *Ichthyornis* and
282 Aves that have a high consistency index including a hypotarsus with grooves and ridges and a
283 medial coracoidal margin that is flat to convex rather than concave with a midline groove
284 otherwise seen in Enantiornithes and more basal avialans (Norell & Clarke, 2001; Clarke, 2004).
285 *Hesperornithes*, *Ichthyornis* and Aves also show a deep medial extensor groove on the tibiotarsus
286 absent in *Apsaravis* (Clarke & Norell, 2002) and an array of other derived states. What is clear is
287 that with the discovery of further diversity in Ornithurae, known homoplasy is also increasing
288 similar to the situation in basal paravian relationships (e.g., Xu et al., 2011).

289

290

291 DISCUSSION

292

293 Jehol Biota continues to reveal important new data on the evolution of morphology in the transition
294 from bipedal terrestrial dinosaurs to volant forms. While character systems tied to locomotor
295 mode have received the most scrutiny, some recent work has begun to address what other changes
296 in ecology and morphology shift as part with this transition, including the gross morphology of the
297 brain (e.g., Balanoff et al., 2014) and cranial shape and ontogeny (Bhullar et al., 2012).

298

299 The presence of feeding ecologies novel for Dinosauria may be expected to be seen within Avialae
300 enabled by evolution of their novel locomotor mode. However, a recent study by using skeletal
301 morphology to predict ecology in both living and extinct birds proposed that the ecological
302 diversity of Cretaceous birds is anomalously low in the Jehol ecosystem and dominated by ground-
303 foraging granivores/insectivores, similar to sparrows or pigeons (Mitchell & Makovicky, 2014).
304 While within living birds, there is enormous diversity in skull shape so far in Mesozoic taxa most
305 diversity has been in dentition (Li et al., 2014), which could be considered one explanation for the
306 low estimates of ecological diversity. Dentition shows complex trends in Avialae including
307 patterns of loss or reduction and evolution of dental morphologies not present in more basal
308 dinosaurs. *Changzuiornis* adds to this known diversity in dentition. The teeth in *Changzuiornis*
309 appear limited to the more posterior portion of dentary, a condition not seen in other birds.
310 Evolution of tooth loss in this clade is proposed to start in the rostral-most part of the premaxillae
311 (Clarke et al., 2006; Louchart & Viriot, 2011). However, there is significant diversity making
312 optimization of ancestral traits largely ambiguous; different dental patterns are distributed as
313 follows: (1) edentulous premaxillary tip (e.g., *Yanornis*, *Yixianornis*); (2) edentulous premaxilla
314 (e.g., *Hesperornis*, *Ichthyornis*, *Gansus zheni*, *Iteravis*, and *Hongshanornis*); (3) edentulous upper
315 jaw (e.g., *Jianchangornis*); (4) edentulous upper jaw and rostral dentary (e.g., *Changzuiornis*); (5)
316 fully edentulous (e.g., *Apsaravis*, *Archaeorhynchus*, *Schizooura*).

317

318 In marked contrast with dentition, so far known diversity in rostral shape in Jehol taxa has been
319 limited (Li et al., 2014); three distinct taxa within ornithurine birds (i.e., *Changzuiornis*,
320 *Hesperornithes*, *Ichthyornis*) show elongate rostri along with one enantiornithurine clade
321 (Longipteryidae; Fig. 4). This rostral shape is rare even in more basal maniraptoran dinosaurs. A
322 developmental explanation of some of these data has been proposed (Bhuller et al., 2012, 2015).
323 Mesozoic birds have plesiomorphic rostral morphologies not seen in extant birds including
324 premaxillae restricted to the tip or cranial half of the facial margin. Recent studies propose
325 peramorphosis in formation of the distinctive elongate avian beak (comprised primarily of
326 premaxilla) phylogenetically between *Confuciusornis* and *Yixianornis*. This shift was
327 hypothesized to be linked to the evolution of the beak into a precise grasping mechanism
328 following increasing specialization of the forelimbs for flight (Bhullar et al., 2012). Supporting
329 the idea of a developmental constraint persisting into basal Ornithurae on rostral development,
330 all Mesozoic taxa with elongate rostra, including *Changzuiornis*, accomplish this elongation
331 through elongation of the maxilla and not the premaxilla (Fig. 4). Given the age and
332 phylogenetic position of the ornithurines that show this morphology, the proposed change in
333 development must occur in the Late Cretaceous, close to the timing of origin for the radiation of
334 all extant birds.

335 The structure and function of the extant avian rostrum in grasping is closely tied to cranial
336 kinesis or zones of mobility or flexure (Bock, 1964; Zusi, 1984). Data from *Changzuiornis* may
337 inform our spotty understanding of this transition. Small vascular foramina (nutrition foramina)
338 are visible on the dorsal surface of the premaxilla, indicating that the anterior margin of the
339 upper jaw was covered by a keratinous sheath or bill. However, as indicated by the
340 comparatively broad nasals, the position of the holorhinal nostril (terminating anterior to the
341 premaxilla/frontal contact), and the loss of teeth in the upper jaw, we think rynchokinesis, the
342 significant proximal and/or distal rostral flexure seen in many extant birds (e.g., cranes, rails,

343 shorebirds, swifts and hummingbirds) may not have been possible (Bock, 1964; Zusi, 1984; Bout
344 & Zweers, 2001; Estrella & Masero, 2007).

345 Prokinesis, in which the upper jaw pivots only at a narrow and well defined craniofacial hinge is
346 widespread in extant birds including galloanserines and has been considered primitive for at least
347 the group including Hesperornithiformes, *Ichthyornis* and Aves given the morphology of the
348 premaxillae-nasofrontal contact in those taxa (Bühler et al., 1988; Witmer, 1995). By contrast, the
349 skull of *Confuciusornis* has been estimated to be only marginally kinetic or akinetic; it exhibits a
350 relatively indistinct naso-frontal zone located approximately on the rostral edge of the cranial
351 vault above part of the orbit (Chiappe et al., 1999; Fig. 4). Unlike *Confuciusornis*, but similar to
352 *Ichthyornis*, *Hesperornis* and extant prokinetic taxa, in *Changzuiornis* the area of contact
353 between the frontals and premaxillae lies anterior to the orbit and is demarcated by zone of
354 dorsal concavity (Fig. 4). The development of an internarial septum in the new species could
355 intuitively limit any more rostral bending (Zusi, 1984). However, the presence of an internarial
356 septum in extant Palaeognathae which exhibit an apparently derived form of rynchokinesis
357 problematizes any simple inference for or against further more rostral flexure (Zusi, 1984;
358 Gussekloo & Bout, 2005). We propose that a form of kinesis may date to at least the common
359 ancestor of *Changzuiornis* and Aves. However we caution that the rostrum of all of these basal
360 taxa is not comprised of only a single bone element but has a prominent juncture in the middle of
361 the facial margin between the small premaxilla and large maxilla that may be expected to affect
362 bending. If Hesperornithes and *Ichthyornis* show a form of prokinesis, as previously proposed,
363 then kinetic demands related to increased grasping function may predate or potentially drive the
364 developmental shift observed.

365 **Conclusions**

366 With its combination of a long and slender bill, proximally- projected cnemial crests, relative
367 long tibiotarsus, and small pedal unguals, *Changzuiornis* represents a distinct departure from
368 other known Jehol birds and contributes to our understanding of morphological and ecological
369 diversity. That highly specialized species usually occur in low numbers (Julliard et al., 2004;
370 Şekercioğlu et al., 2014) in a given fauna, maybe one explanation for comparative paucity of
371 previously known diversity in rostral morphology in the Jehol Biota. At the same time Mesozoic
372 avialans maybe be subject to developmental constraints on rostral shape (Bhullar et al., 2012)
373 and most diversity in feeding ecology is reflected in diversity in dentition. If so, inferences of
374 feeding ecology primarily from rostral shape in Mesozoic birds should be approached with
375 caution (Li et al., 2014). *Changzuiornis* constrains further when this shift in rostral development
376 (Bhullar et al., 2012, 2015) may have occurred. So far it appears to be a Late Cretaceous
377 phenomenon that arose close to the timing of crown clade origin and as such should be further
378 investigated as a possible key innovation in their remarkable radiation. Increased kinesis,
379 possibly as a form of prokinesis, is estimated to predate this developmental shift.

380

381 **ACKNOWLEDGEMENTS**

382 We thank Zhiheng Li for help with the data matrix and Anjan Bhullar, Arhat Abzhanov, and
383 Zack Morris for discussion. The comments of two anonymous referees improved the manuscript.

384

385 **Competing Interests**

386 The authors declare no competing interests.

387 **Author Contributions**

388 X. Wang and J. A. Clarke designed the study collected, analyzed data, prepared figures and
389 wrote the manuscript. J. Peteya analyzed feather color data. J. Huang, Y. Hu and J. Liu provided
390 study materials and assistance with the locality data for the paper.

391

392 **REFERENCES**

- 393 **Balanoff AM, Bever G, Norell MA. 2014.** Reconsidering the avian nature of the oviraptorosaur
394 brain (Dinosauria: Theropoda). *Plos One* **9**:e113559.
- 395 **Bhullar B-AS, Marugán-Lobón J, Racimo F, Bever GS, Rowe TB, Norell MA, Abzhanov A.**
396 **2012.** Birds have paedomorphic dinosaur skulls. *Nature* **487**:223-226.
- 397 **Bhullar B-AS, Morris ZS, Sefton EM, Tok A, Tokita M, Namkoong B, Camacho J,**
398 **Burnham DA, Abzhanov A. 2015.** A molecular mechanism for the origin of a key
399 evolutionary innovation, the bird beak and palate, revealed by an integrative approach to
400 major transitions in vertebrate history. *Evolution* **69**: 1665–1677. doi: 10.1111/evo.12684
- 401 **Bock WJ. 1964.** Kinetics of the avian skull. *Journal of morphology* **114**:1-41.
- 402 **Bout RG, Zweers GA. 2001.** The role of cranial kinesis in birds. *Comparative Biochemistry and*
403 *Physiology Part A: Molecular & Integrative Physiology* **131(1)**: 197-205.
- 404 **Bühler P, Martin LD, Witmer LM. 1988.** Cranial kinesis in the Late Cretaceous birds
405 *Hesperornis* and *Parahesperornis*. *The Auk*, 111-122.
- 406 **Chang S-c, Zhang H, Renne PR, Fang Y. 2009.** High-precision 40 Ar/39 Ar age for the Jehol
407 biota. *Palaeogeography, Palaeoclimatology, Palaeoecology* **280**:94-104.
- 408 **Chiappe LM, Ji SA, Ji Q, Norell MA. 1999.** Anatomy and systematics of the
409 Confuciusornithidae (Theropoda, Aves) from the late Mesozoic of northeastern China.
410 *Bulletin of the AMNH*; no. 242.
- 411 **Chiappe LM, Zhao B, O'Connor JK, Chunling G, Wang X, Habib M, Marugan-Lobon J,**
412 **Meng Q, Cheng X. 2014.** A new specimen of the Early Cretaceous bird *Hongshanornis*
413 *longicresta*: insights into the aerodynamics and diet of a basal ornithuromorph. *PeerJ*
414 **2**:e234.
- 415 **Clarke JA. 2004.** Morphology, phylogenetic taxonomy, and systematics of *Ichthyornis* and
416 *Apatornis* (Avialae: Ornithurae). *Bulletin of the American Museum of Natural History*:1-
417 179.
- 418 **Clarke JA, Norell MA. 2002.** The morphology and phylogenetic position of *Apsaravis ukhaana*
419 from the Late Cretaceous of Mongolia. *American Museum Novitates* 1-46.
- 420 **Clarke JA, Zhou Z, Zhang F. 2006.** Insight into the evolution of avian flight from a new clade
421 of Early Cretaceous ornithurines from China and the morphology of *Yixianornis grabaui*.
422 *Journal of anatomy* **208**:287-308.
- 423 **Clarke JA, Ksepka DT, Salas-Gismondi R, Altamirano AJ, Shawkey MD, D'Alba L, ...**
424 **Baby P. 2010.** Fossil evidence for evolution of the shape and color of penguin
425 feathers. *Science* **330(6006)**: 954-957.

- 426 **Estrella SM, Masero JA. 2007.** The use of distal rynchokinesis by birds feeding in
427 water. *Journal of Experimental Biology* **210(21)**:3757-3762.
- 428 **Forster CA, Sampson SD, Chiappe LM, Krause DW. 1998.** The theropod ancestry of birds:
429 New evidence from the Late Cretaceous of Madagascar. *Science* **279**:1915-1919.
- 430 **Gao C, Chiappe LM, Zhang F, Pomeroy DL, Shen C, Chinsamy A, Walsh MO. 2012.** A
431 subadult specimen of the Early Cretaceous bird *Sapeornis chaoyangensis* and a
432 taxonomic reassessment of sapeornithids. *Journal of Vertebrate Paleontology* **32**:1103-
433 1112.
- 434 **Gauthier J, De Queiroz K. 2001.** Feathered dinosaurs, flying dinosaurs, crown dinosaurs, and
435 the name "Aves". *New Perspectives on the Origin and Early Evolution of Birds*:7-41.
- 436 **Gingerich P. 1973.** Skull of Hesperornis and early evolution of birds. *Nature* **243**:70-73.
- 437 **Godefroit P, Demuynck H, Dyke G, Hu D, Escuillie F, Claeys P. 2013.** Reduced plumage and
438 flight ability of a new Jurassic paravian theropod from China. *Nature Communications*
439 **4**:1394.
- 440 **Gussekklo SW, Bout RG. 2005.** The kinematics of feeding and drinking in palaeognathous birds
441 in relation to cranial morphology. *Journal of Experimental Biology* **208(17)**: 3395-3407.
- 442 **Haeckel EH. 1866.** Generelle morphologie der organismen. Berlin: Georg Reimer, 462.
- 443 **Hieronymus Tobin L. 2015.** Qualitative skeletal correlates of wing shape in extant birds (Aves:
444 Neoaves). *BMC evolutionary biology* **15**: 30.
- 445 **Hou L. 1997.** *Mesozoic Birds of China*. Taiwan Provincial Feng Huang Ku Bird Park. Taiwan,
446 Nan Tou. i0003-0082.
- 447 **Hou L, Chiappe LM, Zhang F, Chuong C-M. 2004.** New Early Cretaceous fossil from China
448 documents a novel trophic specialization for Mesozoic birds. *Naturwissenschaften* **91**:22-
449 25.
- 450 **Julliard R, Jiguet F, Couvet D. 2004.** Common birds facing global changes: what makes a
451 species at risk? *Global Change Biology* **10(1)**:148-154.
- 452 **Li Q, Gao KQ, Vinther J, Shawkey MD, Clarke JA, D'alba L, ... Prum R O. 2010.** Plumage
453 color patterns of an extinct dinosaur. *Science* **327(5971)**: 1369-1372.
- 454 **Li Z, Zhou Z, Wang M, Clarke JA. 2014.** A new specimen of large-bodied basal
455 enantiornithine *Bohaiornis* from the Early Cretaceous of China and the inference of
456 feeding ecology in Mesozoic birds. *Journal of Paleontology* **88**:99-108.
- 457 **Liu D, Chiappe LM, Zhang Y, Bell A, Meng Q, Ji Q, Wang X. 2014.** An advanced, new long-
458 legged bird from the Early Cretaceous of the Jehol Group (northeastern China): insights
459 into the temporal divergence of modern birds. *Zootaxa* **3884**:253-266.
- 460 **Louchart A, Viriot L. 2011.** From snout to beak: the loss of teeth in birds. *Trends in Ecology &*
461 *Evolution* **26**:663-673.
- 462 **Martin LD. 2011.** The other half of avian evolution: Cyril Walker's contribution. *Journal of*
463 *Systematic Palaeontology* **9(1)**: 3-8.
- 464 **Marsh OC. 1880.** *Odontornithes: a monograph on the extinct toothed birds of North*
465 *America* Washington, DC:Government Printing Office.
- 466 **Mitchell JS, Makovicky PJ. 2014.** Low ecological disparity in Early Cretaceous birds.
467 *Proceedings of the Royal Society B: Biological Sciences* **281**:20140608.
- 468 **Nudds R, Atterholt J, Wang X, You HL, Dyke G. 2013.** Locomotory abilities and habitat of
469 the Cretaceous bird *Gansus yumenensis* inferred from limb length proportions. *Journal of*
470 *Evolutionary Biology* **26**:150-154.

- 471 **O'Connor JK, Gao K-Q, Chiappe LM. 2010.** A new ornithuromorph (Aves: Ornithothoraces)
472 bird from the Jehol Group indicative of higher-level diversity. *Journal of Vertebrate*
473 *Paleontology* **30**:311-321.
- 474 **O'Connor JK, Wang X, Chiappe LM, Gao C, Meng Q, Cheng X, Liu J. 2009.** Phylogenetic
475 support for a specialized clade of Cretaceous enantiornithine birds with information from
476 a new species. *Journal of Vertebrate Paleontology* **29**:188-204.
- 477 **O'Connor JK, Chiappe LM. 2011.** A revision of enantiornithine (Aves: Ornithothoraces) skull
478 morphology. *Journal of Systematic Palaeontology* **9(1)**: 135-157.
- 479 **Şekerciöglu ÇH, Daily GC, Ehrlich PR. 2004.** Ecosystem consequences of bird
480 declines. *Proceedings of the National Academy of Sciences* **101(52)**: 18042-18047.
- 481 **Suarez MB, Ludvigson GA, González LA, Al-Suwaidi AH, You H-L. 2013.** Stable isotope
482 chemostratigraphy in lacustrine strata of the Xiagou Formation, Gansu Province, NW
483 China. *Geological Society, London, Special Publications* **382**:SP382. 381.
- 484 **Swofford DL. 2003.** PAUP*. Phylogenetic analysis using parsimony (* and other methods).
485 Version 4.
- 486 **Turner AH, Pol D, Clarke JA, Erickson GM, Norell MA. 2007.** A basal dromaeosaurid and
487 size evolution preceding avian flight. *Science* **317**:1378-1381.
- 488 **Vinther J, Briggs DE, Clarke J, Mayr G, Prum RO. 2009.** Structural coloration in a fossil
489 feather. *Biology Letters* 20090524.
- 490 **Wang M, Zheng X, O'Connor JK, Lloyd GT, Wang X, Wang Y, Zhou Z. 2015.** The oldest
491 record of ornithuromorpha from the early cretaceous of China. *Nature*
492 *communications*, **6**. 6987 doi: 10.1038/ncomms7987
- 493 **Wang X, Chiappe ML, Teng F, Ji Q. 2013.** *Xinghaiornis lini* (Aves: Ornithothoraces) from the
494 Early Cretaceous of Liaoning: An example of evolutionary mosaic in early birds. *Acta*
495 *Geologica Sinica* (English edition) **87(3)**: 686-689.
- 496 **Witmer LM. 1995.** Homology of
497 facial structures in extant archosaurs (birds and crocodylians), with special reference to
498 paranasal pneumaticity and nasal conchae. *Journal of morphology* **225**:269-327.
- 499 **Xu X, Norell MA. 2004.** A new troodontid dinosaur from China with avian-like sleeping
500 posture. *Nature* **431**:838-841.
- 501 **Xu X, You H, Du K, Han F. 2011.** An *Archaeopteryx*-like theropod from China and the origin
502 of Avialae. *Nature* **475(7357)**: 465-470.
- 503 **You H-l, Lamanna MC, Harris JD, Chiappe LM, O'Connor J, Ji S-a, Lu J-c, Yuan C-x, Li**
504 **D-q, Zhang X, Lacovara KJ, Dodson P, Ji Q. 2006.** A nearly modern amphibious bird
505 from the Early Cretaceous of northwestern China. *Science* **312**:1640-1643.
- 506 **Zheng X, Martin LD, Zhou Z, Burnham DA, Zhang F, Miao D. 2011.** Fossil evidence of
507 avian crops from the Early Cretaceous of China. *Proceedings of the National Academy of*
508 *Sciences* **108**:15904-15907.
- 509 **Zheng X, O'Connor J, Wang X, Zhang X, Wang Y. 2014.** New Information on
510 Hongshanornithidae (Aves: Ornithuromorpha) from a new subadult specimen. *Vertebrata*
511 *Palasiatica* **52**:16.
- 512 **Zhou S, O'Connor JK, Wang M. 2014a.** A new species from an ornithuromorph (Aves:
513 Ornithothoraces) dominated locality of the Jehol Biota. *Chinese Science Bulletin*
514 **59**:5366-5378.
- 515 **Zhou S, Zhou Z, O'Connor J. 2014b.** A new piscivorous ornithuromorph from the Jehol Biota.
Historical Biology **26**:608-618.

- 516 **Zhou S, Zhou Z, O'Connor J. 2012.** A new toothless ornithurine bird (*Schizooura lii* gen. et sp.
517 nov.) from the Lower Cretaceous of China. *Vertebrata Palasiatica* **50**:9-24.
- 518 **Zhou S, Zhou Z, O'Connor JK. 2013.** Anatomy of the basal ornithuromorph bird
519 *Archaeorhynchus spathula* from the Early Cretaceous of Liaoning, China. *Journal of*
520 *Vertebrate Paleontology* **33**:141-152.
- 521 **Zhou Z, Clarke J, Zhang F. 2008.** Insight into diversity, body size and morphological evolution
522 from the largest Early Cretaceous enantiornithine bird. *Journal of anatomy* **212**:565-577.
- 523 **Zhou Z, Clarke J, Zhang F, Wings O. 2004.** Gastroliths in *Yanornis*: an indication of the
524 earliest radical diet-switching and gizzard plasticity in the lineage leading to living birds?
525 *Naturwissenschaften* **91**:571-574.
- 526 **Zhou Z, Zhang F. 2001.** Two new ornithurine birds from the Early Cretaceous of western
527 Liaoning, China. *Chinese Science Bulletin* **46**:1258-1264.
- 528 **Zhou Z, Zhang F. 2005.** Discovery of an ornithurine bird and its implication for Early
529 Cretaceous avian radiation. *Proceedings of the National Academy of Sciences of the*
530 *United States of America* **102**:18998-19002.
- 531 **Zhou Z, Zhang F. 2006.** A beaked basal ornithurine bird (Aves, Ornithurae) from the Lower
532 Cretaceous of China. *Zoologica Scripta* **35**:363-373.
- 533 **Zhou Z, Zhang F, Li Z. 2009.** A new basal ornithurine bird (*Jianchangornis microdonta* gen. et
534 sp. nov.) from the Lower Cretaceous of China. *Vertebrata Palasiatica* **47**:299-310.
- 535 **Zusi RL. 1984.** *A functional and evolutionary analysis of rhynchokinesis in birds*: Citeseer.

536

537

538

539

540

541

542

543

544 **Figure Captions**

545

546 **Fig.1 Distribution of Ornithurae birds from Early Cretaceous of China.** So far more than 14
 547 species of ornithurine birds have been reported from multiple locations of the Early Cretaceous of
 548 northern China, Jehol Biota (i.e., *Songlingornis linghensis*, *Chaoyangia beishanensis*, *Yanornis*
 549 *martini*, *Yixianornis grabaui*, *Gansus yumenensis*, *Hongshanornis longicresta*, *Archaeorhynchus*
 550 *spathula*, *Longicrusavis houi*, *Parahongshanornis chaoyangensis*, *Tianyuornis cheni*,
 551 *Archaeornithura meemanna*, *Jianchangornis microdonta*, *Schizooura lii*, *Piscivoravis lii*, *Iteravis*
 552 *huchzermeyeri*, *Gansus zheni*, *Xinghaiornis lini*; Hou, 1997; Zhou & Zhang, 2001; Zhou & Zhang,
 553 2005; Clarke et al., 2006; You et al., 2006; Zhou & Zhang, 2006; Zhou et al., 2009; O'Connor et
 554 al., 2010; Zhou et al., 2012; Zhou et al., 2013; Wang et al., 2013; Chiappe et al., 2014; Liu et al.,
 555 2014; Zheng et al., 2014; Zhou et al., 2014a; Zhou et al., 2014b; Wang et al., 2015).

556

557 **Fig.2 Photograph of the Holotype *Changzuiornis ahgm* (AGB5840).** Anatomical abbreviations:
 558 co, coracoid; cv, cervical vertebra; f, feathers; fe, femur; fu, furcula; ga, gastrolith; hu, humerus;
 559 il, ilium; ins, internarial septum; ios, interorbital septum; mcI–III, metacarpals I–III; pd I–IV, pedal
 560 digits I–IV; phI-1, the first phalanx of digit I; phI-2, the second phalanx of digit I; phII-1, the first
 561 phalanx of digit II; phII-2, the second phalanx of digit II; pu, pubis; py, pygostyle; ra, radius; rad,
 562 radiale; ri, rib; sc, scapula; sk, skull; ti, tibiotarsus; tm, tarsometatarsus; tv, thoracic vertebra; ul,
 563 ulna; uln, ulnare. Numbers (1, 2) show the locations of SEM imaging of feather remains. Insets
 564 show melanosome morphologies from the two sample locations.

565

566 **Fig.3 Skull of *Changzuiornis ahgm*.** Anatomical abbreviations: bh, basihyal; ce, ceratobranchial;
 567 de, dentary; fp, frontal process; fpc, frontals and premaxillae contacting area; fr, frontal; ins,
 568 internarial septum; la, lacrimal; ma, maxilla; na, nasal; pa, parietal; pd, prementary; pm,
 569 premaxillae; q, quadrate. Inset showing the tiny teeth preserved on dentary.

570

571 **Fig.4 Close-up of the skull of *Changzuiornis ahgm*.** Anatomical abbreviations: atm, articulating
 572 tip of the maxilla; dpm, dorsal process of the maxilla; en, external nares; fd, forked dentary; fp,
 573 frontal process; fpc, frontals and premaxillae contacting area; ins, internarial septum; ios,
 574 interorbital septum; lfp, left frontal process; os, scleral ossicles.

575

576 **Fig.5 Pectoral girdle and forelimb of *Changzuiornis ahgm*.** Anatomical abbreviations: ap,
 577 acromion process; co, coracoid; dc, deltopectoral crest; fu, furcula; h, head; hu, humerus; lp, lateral
 578 process; pp, procoracoid process; rad, radii; ri, rib; sc, scapula; uln, ulnae.

579

580 **Fig. 6 Carpometacarpus of *Changzuiornis ahgm*.** Anatomical abbreviations: ep, extensor
 581 process; fo, fossa; im, impression; mcI–III, metacarpals I–III; phI-1, the first phalanx of digit I;
 582 phI-2, the second phalanx of digit I; phII-1, the first phalanx of digit II; phII-2, the second phalanx
 583 of digit II; phII-3, the third phalanx of digit II; pip, piciform process; ra, radius; ul, ulna.

584

585 **Fig.7 Pelvic girdle of *Changzuiornis ahgm*.** Anatomical abbreviations: cc, cnemial crest; fcl,
 586 fovea for capital ligament; fe, femur; pu, pubis; sy, symphysis; tc, trochanteric crest; tct, tibialis
 587 cranialis tubercle; ti, tibiotarsus; tm, tarsometatarsus.

588

589 **Fig.8 Strict consensus cladogram illustrating the phylogenetic position of *Changzuiornis***
590 ***ahgm.*** [length L: 585, CI: 0.50, RI 0.79, RC 0.40 (PIC only)]. Bootstrap support for those nodes
591 recovered in greater than 50% of the 1000 replicates performed and Bremer (1988) support
592 values are reported to the right of the node to which they apply (Format: Bootstrap/Bremer).
593 Skulls are illustrated to show the change of facial margin composition along the evolution of
594 avialans. Red, maxilla; yellow, premaxilla. The skull of *Rapaxavis* (Longipterygidae) with
595 elongated rostrum is also shown here.

Table 1 (on next page)

Measurements of the new specimens referred to *Changzuiornis angmi* (AGB5840)

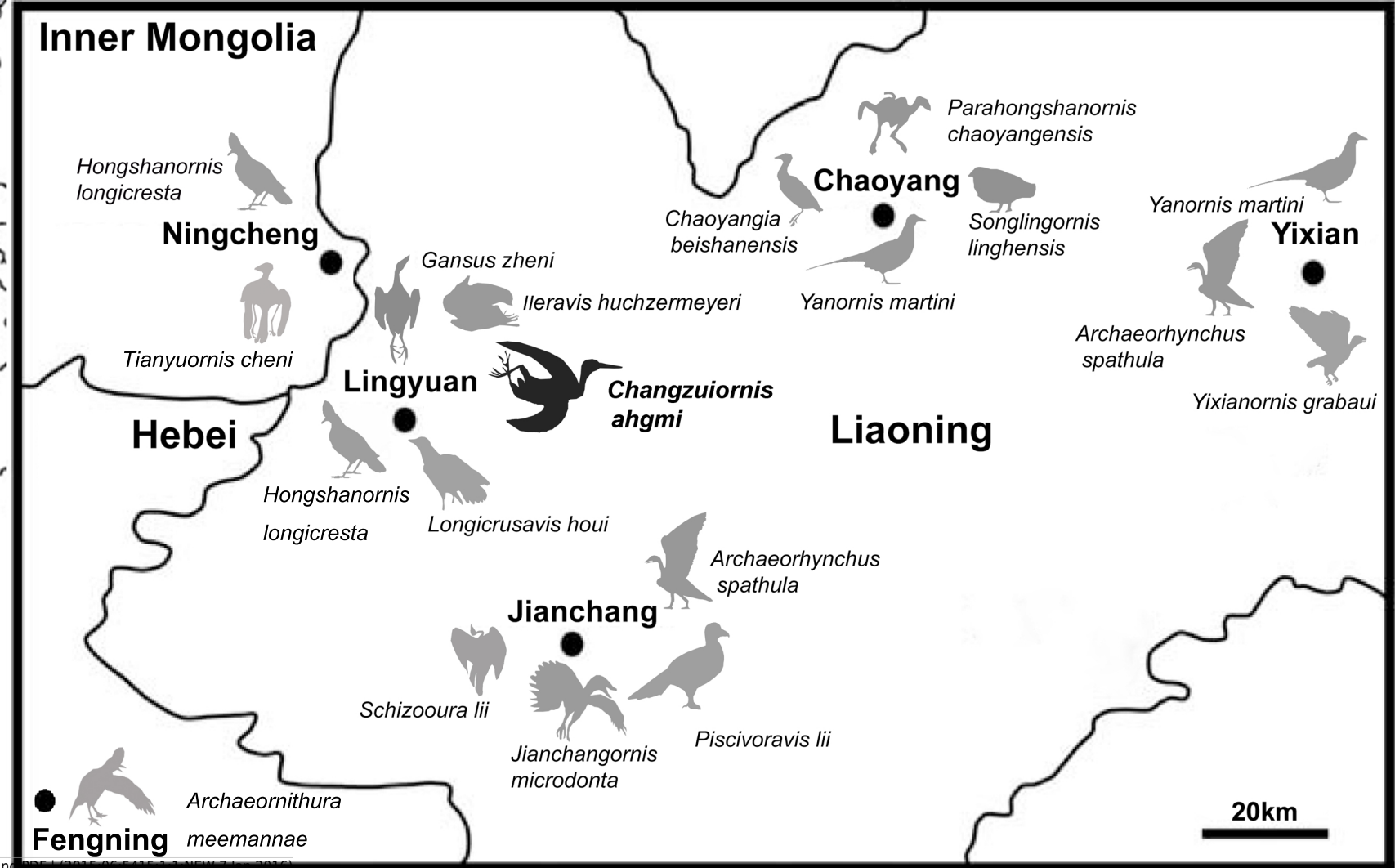
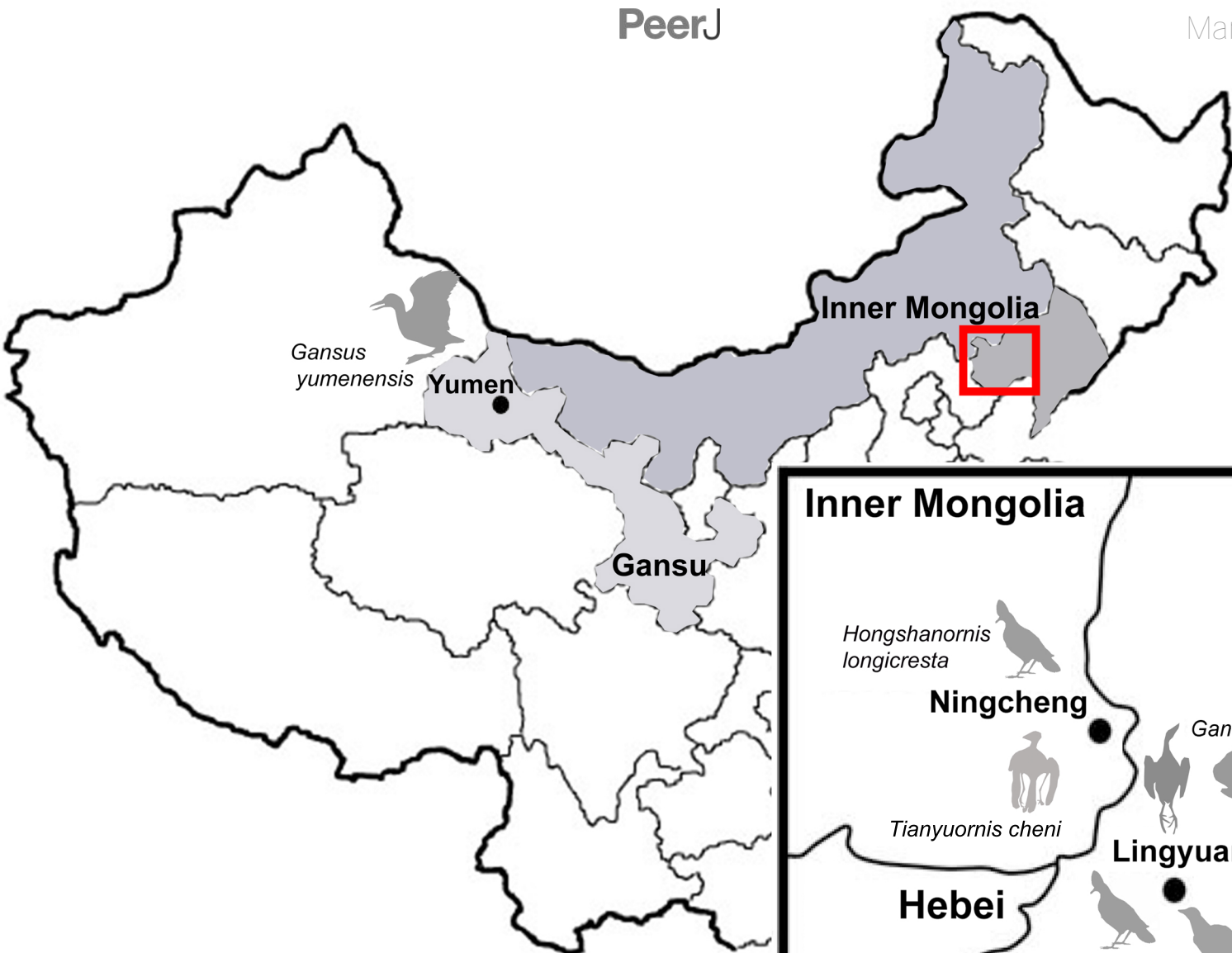
Table 1 Measurements of the new specimens referred to *Changzuornis angmi* (AGB5840) (in cm) L/R

Premaxilla length along facial margin	3.22	Phalanx II:3	0.36
Dentary length, total	5.48	Phalanx III:1	-
Rostrum length (from the tip of premaxilla to frontal and premaxilla contact)	4.80	Ilium length total	3.04
Dentary dorsoventral height at anterior tip	0.11	Ilium preacetabular	1.43
Cervical vertebra average length	0.71	Ischium length	3.84*
Sacrum length	3.3*	Pubis length	3.43
Sternum length on midline	-	Pubis average shaft diameter	0.21
Scapula maximum length	4.64R	Pubis symphysis length	1.35
Coracoid height	2.38R	Pelvic limb	
Coracoid sternal margin length	-	Femur maximum length	2.94R
Coracoidal lateral process length	1.19R	midshaft width	0.35
		Tibia maximum length,	
Furcula: length clavicular ramus	1.67	not including cnemial crest	5.37/5.40
Humerus maximum length	5.04/5.01	Tarsometatarsus maximum length	3.60/3.61
Radius length	5.06/4.86	Pedal phalanx I:1 length	0.72R
Radius midshaft width	0.25/0.23	Pedal phalanx II:1	0.95/0.87
Ulna length	5.2/0.36	Pedal phalanx II:2	1.07/0.99
Ulna midshaft width	0.4/0.36	Pedal phalanx III:1	0.89/0.71
Carpometacarpus maximum length	2.88/3.13	Pedal phalanx III:2	0.84/0.68
Metacarpal I length	0.54/0.76	Pedal phalanx III:3	0.59*/0.63
Metacarpal III width	0.14/0.14	Pedal phalanx IV:1	0.77/0.74
Metacarpal II width	0.22/0.32	Pedal phalanx IV:2	0.72/0.71
Manual phalanx I:1	1.17	Pedal phalanx IV:3	0.54/0.60
Manual Phalanx I:2	0.54R	Pedal phalanx IV:4	0.54/0.65
		Remiges: maximum length distal	
Manual Phalanx II:1	1.29/1.16	primaries (9 & 8?)	15.36
Manual Phalanx II:2	1.44/1.26		

* estimated; L, left; R, right.

Figure 1(on next page)**Distribution of Ornithurae birds from Early Cretaceous of China.**

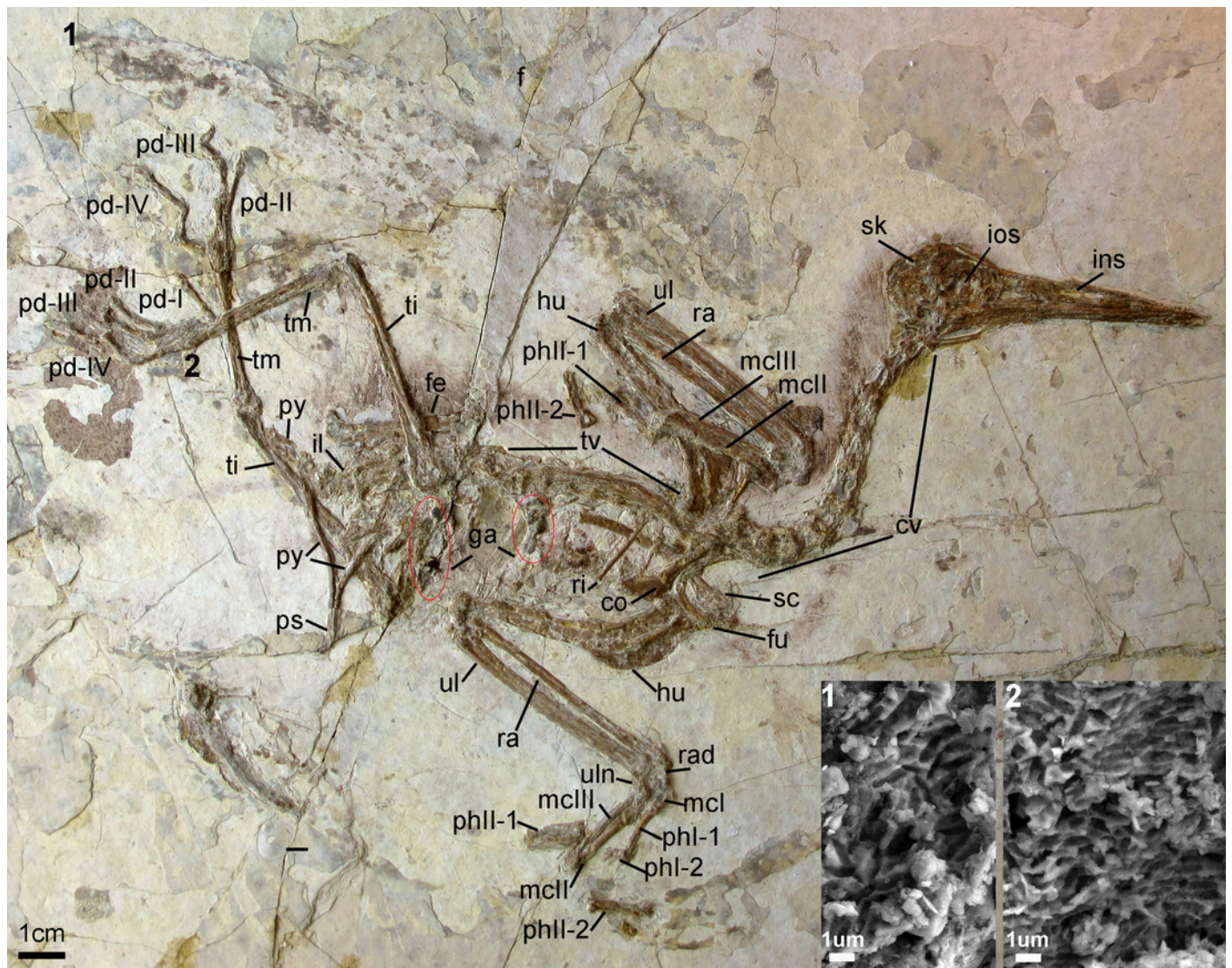
So far more than 14 species of ornithurine birds have been reported from multiple locations of the Early Cretaceous of northern China, Jehol Biota (i.e., *Songlingornis linghensis* , *Chaoyangia beishanensis* , *Yanornis martini* , *Yixianornis grabau* , *Gansus yumenensis* , *Hongshanornis longicresta* , *Archaeorhynchus spathula* , *Longicrusavis houi* , *Parahongshanornis chaoyangensis* , *Tianyuornis cheni*, *Archaeornithura meemanna*, *Jianchangornis microdonta* , *Schizooura lii* , *Piscivoravis lii*, *Iteravis huchzermeyeri*, *Gansus zheni*, *Xinghaiornis lini* ; Hou, 1997 ; Zhou & Zhang, 2001 ; Zhou & Zhang, 2005 ; Clarke et al., 2006 ; You et al., 2006 ; Zhou & Zhang, 2006 ; Zhou et al., 2009 ; O'Connor et al., 2010 ; Zhou et al., 2012 ; Zhou et al., 2013 ; Wang et al., 2013; Chiappe et al., 2014 ; Liu et al., 2014 ; Zheng et al., 2014 ; Zhou et al., 2014a ; Zhou et al., 2014b ; Wang et al., 2015) .



2

Fig.2 Photograph of the Holotype *Changzuornis ahgm* (AGB5840).

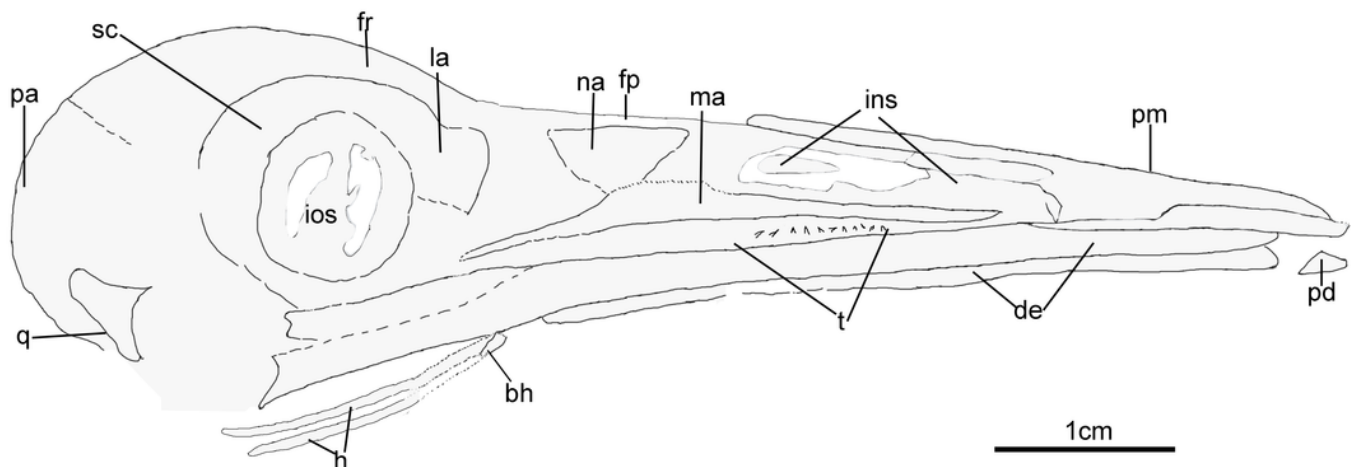
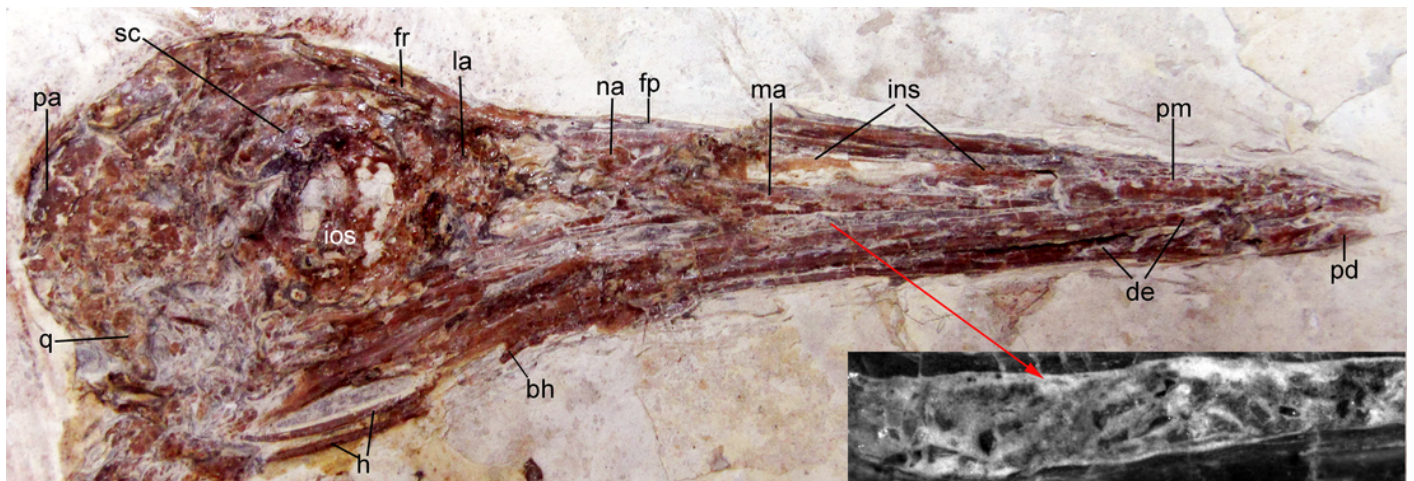
Anatomical abbreviations: co, coracoid; cv, cervical vertebra; f, feathers; fe, femur; fu, furcula; ga, gastrolith; hu, humerus; il, ilium; ins, internarial septum; ios, interorbital septum; mcl-III, metacarpals I-III; pd I-IV, pedal digits I-IV; phi-1, the first phalanx of digit I; phi-2, the second phalanx of digit I; phll-1, the first phalanx of digit II; phll-2, the second phalanx of digit II; pu, pubis; py, pygostyle; ra, radius; rad, radiale; ri, rib; sc, scapula; sk, skull; ti, tibiotarsus; tm, tarsometatarsus; tv, thoracic vertebra; ul, ulna; uln, ulnare . Numbers (1, 2) show the locations of SEM imaging of feather remains. Insets show melanosome morphologies from the two sample locations.



3

Skull of *Changzuornis ahgm.*

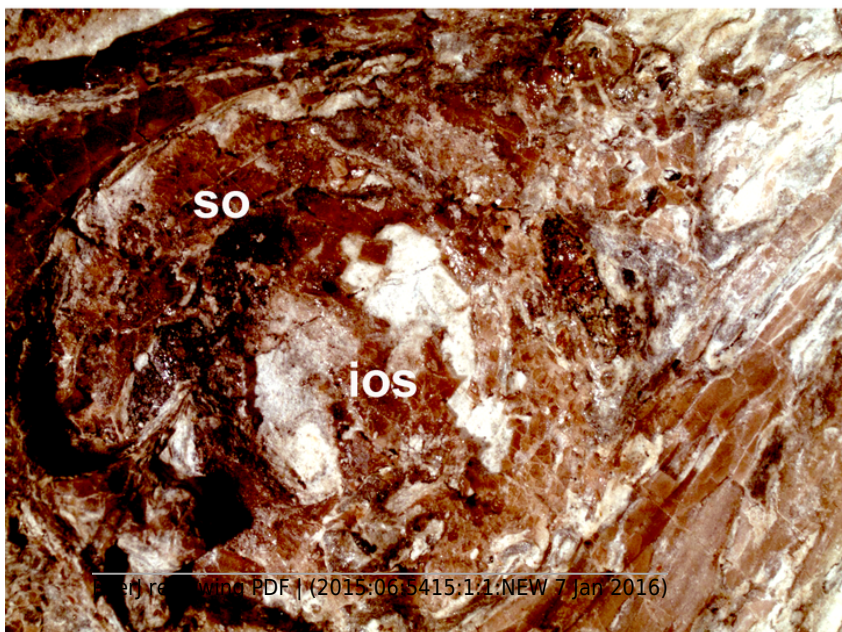
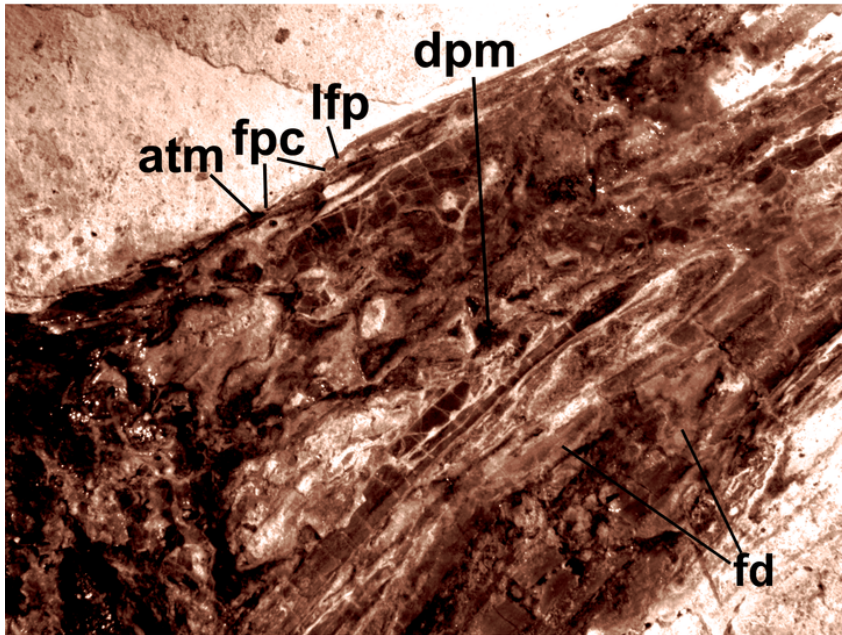
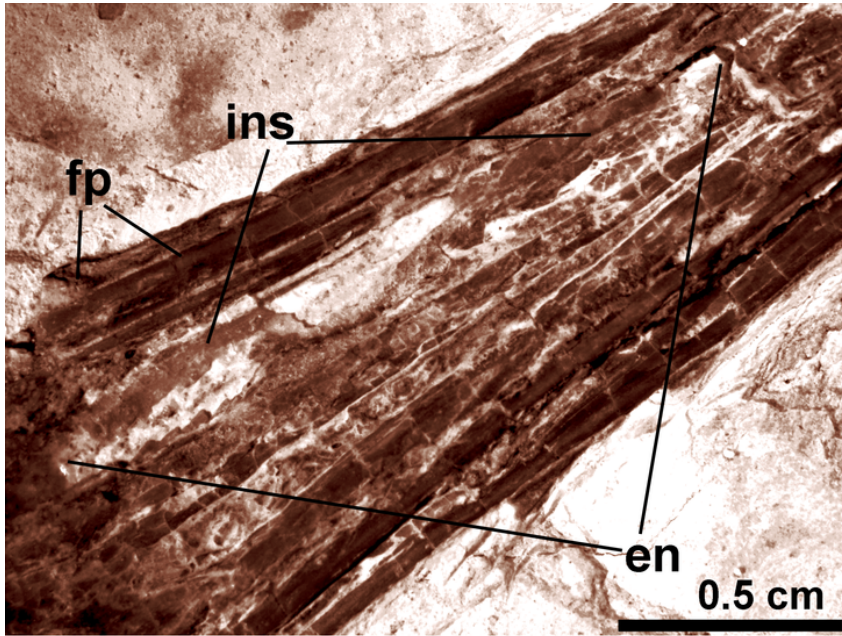
Anatomical abbreviations: bh, basihyal; ce, ceratobranchial; de, dentary; fp, frontal process; fpc, frontals and premaxillae contacting area; fr, frontal; ins, internarial septum; la, lacrimal; ma, maxilla; na, nasal; pa, parietal; pd, prementary; pm, premaxillae; q, quadrate. Inset showing the tiny teeth preserved on dentary.



4

Close-up of the skull of *Changzuornis ahgm*.

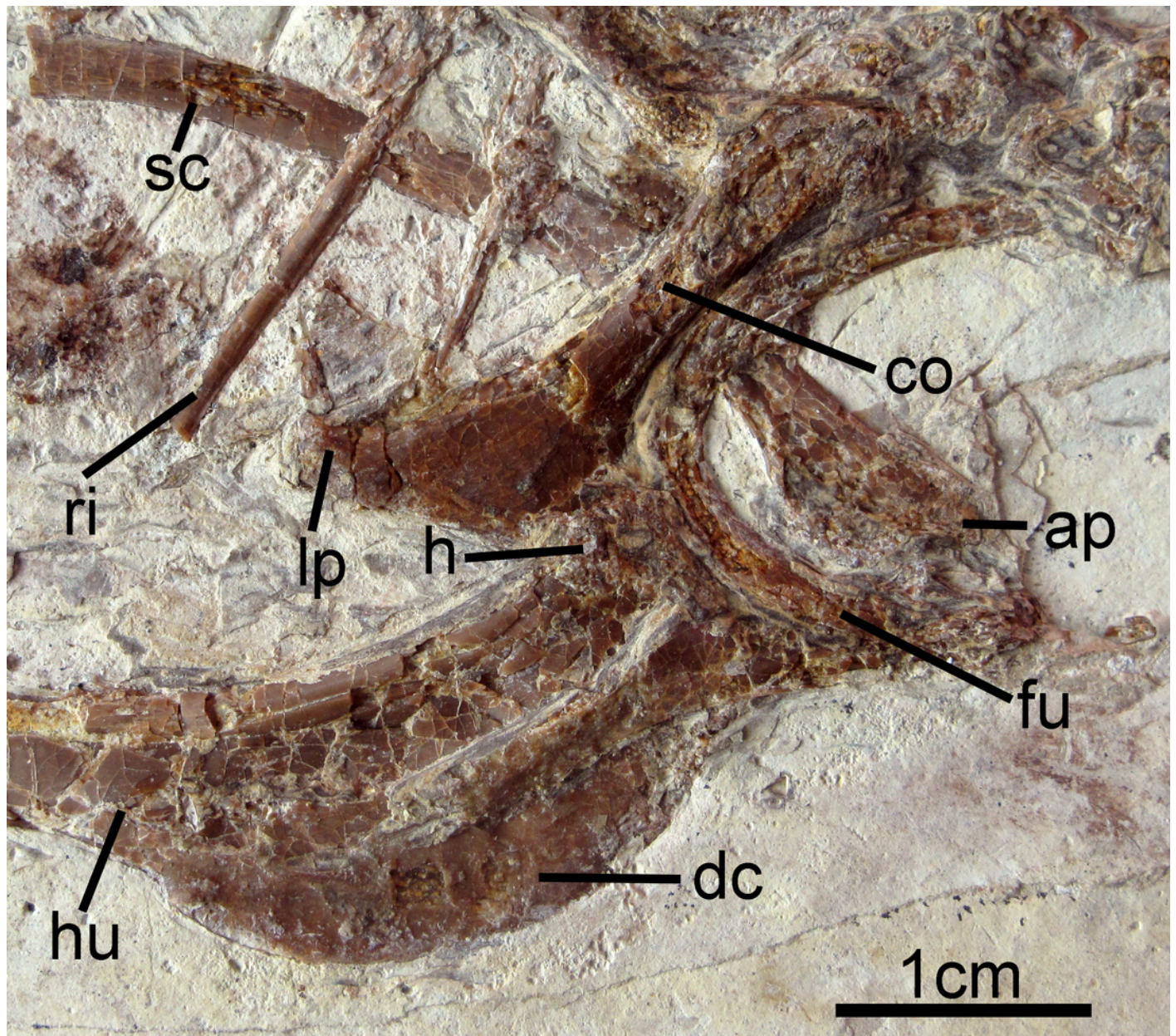
Anatomical abbreviations: atm, articulating tip of the maxilla; dpm, dorsal process of the maxilla; en, external nares; fd, forked dentary; fp, frontal process; fpc, frontals and premaxillae contacting area; ins, internarial septum; ios, interorbital septum; lfp, left frontal process; os, scleral ossicles.



5

Pectoral girdle and forelimb of *Changzuornis ahgm.*

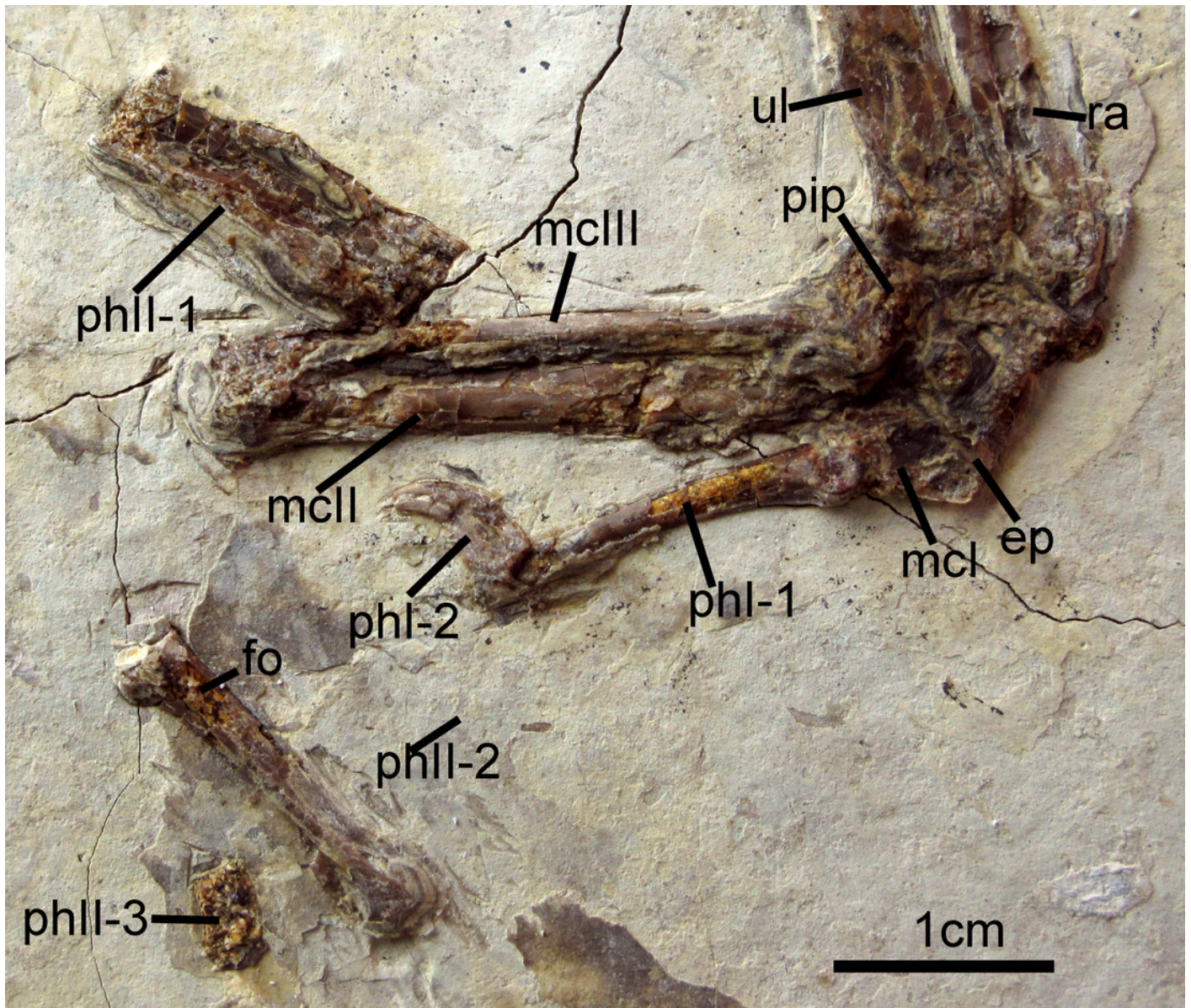
Anatomical abbreviations: atm, articulating tip of the maxilla; dpm, dorsal process of the maxilla; en, external nares; fd, forked dentary; fp, frontal process; fpc, frontals and premaxillae contacting area; ins, internarial septum; ios, interorbital septum; lfp, left frontal process; os, scleral ossicles.



6

Carpometacarpus of *Changzuiornis ahgm.*

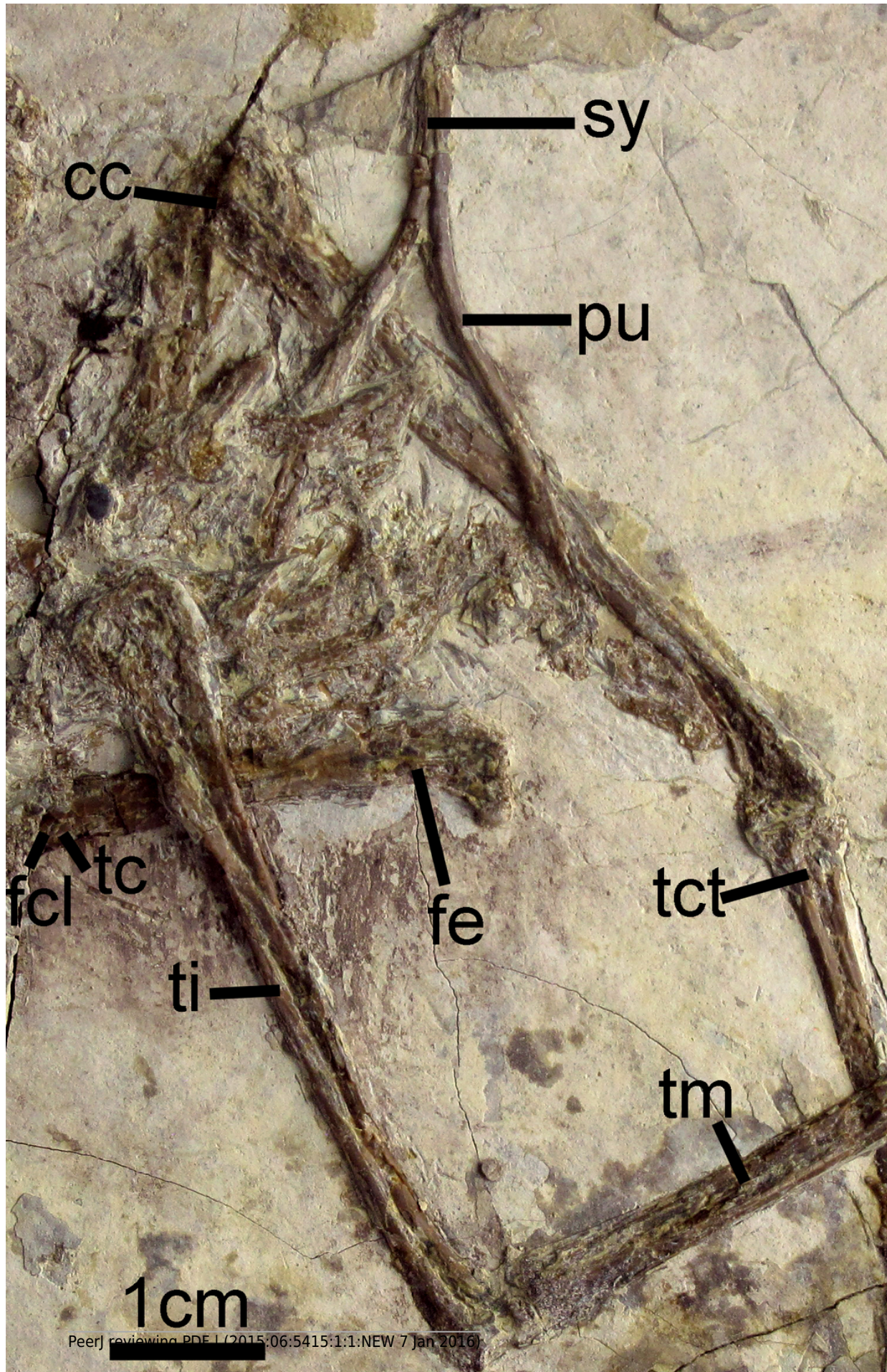
Anatomical abbreviations: ep, extensor process; fo, fossa; im, impression; mcl-I-III, metacarpals I-III; phl-1, the first phalanx of digit I; phl-2, the second phalanx of digit I; phll-1, the first phalanx of digit II; phll-2, the second phalanx of digit II; phll-3, the third phalanx of digit II; pip, piciform process; ra, radius; ul, ulna.



7

Pelvic girdle of *Changzuornis ahgm.*

Anatomical abbreviations: cc, cnemial crest; fcl, fovea for capital ligament; fe, femur; pu, pubis; sy, symphysis; tc, trochanteric crest; tct, tibialis cranialis tubercle; ti, tibiotarsus; tm, tarsometatarsus.



8

Strict consensus cladogram illustrating the phylogenetic position of *Changzuiornis ahgm* .

[length L: 585, CI: 0.50, RI 0.79, RC 0.40 (PIC only)]. Bootstrap support for those nodes recovered in greater than 50% of the 1000 replicates performed and Bremer (1988) support values are reported to the right of the node to which they apply (Format: Bootstrap/Bremer). Skulls are illustrated to show the change of facial margin composition along the evolution of avialans. Red, maxilla; yellow, premaxilla. The skull of *Rapaxavis* (Longipterygidae) with elongated rostrum is also shown here.

